

# Two dimensional quantum central limit theorem by quantum walks

Keisuke Asahara,<sup>1</sup> Daiju Funakawa,<sup>2</sup> Motoki Seki,<sup>3</sup> and Akito Suzuki<sup>4</sup>

<sup>1</sup>*Data Science and AI Innovation Research Center,  
Shiga University, 1-1-1 Banba hikone, Shiga 522-8522, Japan\**

<sup>2</sup>*Department of Electronics and Information Engineering,  
Hokkai-Gakuen University. Sapporo, Hokkaido 062-8605, Japan†*

<sup>3</sup>*Department of Mathematics, Faculty of Science, Hokkaido University, Sapporo, 060-0810, Japan‡*

<sup>4</sup>*Department of Production Systems Engineering and Sciences, Komatsu University,  
Awazu Campus, Nu 1-3 Shicho-machi, Komatsu, Ishikawa 923-8511, Japan§*

Quantum walks, mathematical models referred to as the quantum counterparts of random walks, have garnered significant attention in recent years with the advancement of quantum computing. The weak limit theorem for quantum walks, analogous to the central limit theorem for random walks, is one of the most important theorems in this field. In this study, we investigated the weak limit theorem for a two-state discrete-time quantum walk on a two-dimensional square lattice. As a result, we derived a two-dimensional probability distribution whose support is the intersection of two ellipses. The probability distribution we obtained resembles the distribution of one-dimensional quantum walks while possessing a unique form specific to two dimensions.

## I. INTRODUCTION

In recent years, quantum walks (QWs), which are the quantum counterparts of random walks, have received considerable attention due to advances in quantum computing [1, 2]. Quantum walks can be broadly classified into two types: discrete-time quantum walks, which involve evolution in distinct steps, and continuous-time quantum walks, which evolve smoothly over time. Our research focuses on the discrete-time type. A fundamental topic of interest within quantum walks is the weak limit theorem, which is analogous to the central limit theorem for classical random walks. The weak limit theorems for one-dimensional quantum walks have been extensively studied [3–11], and in most cases, the probability distribution of one-dimensional quantum walks is described by a distribution known as the Konno distribution, given by

$$f_K(v; r) = \frac{\sqrt{1-r^2}}{\pi(1-v^2)\sqrt{r^2-v^2}} I_{(-r,r)}(v), \quad (1)$$

where  $I_S(v)$  is indicator function of a set  $S$ . In contrast, the weak limit theorems for two-dimensional quantum walks have not been fully investigated. Watabe *et al.* [12] and Di Franco *et al.* [13] analytically studied two-dimensional four-state generalized Grover walk, and obtained the following probability distribution:

$$f(v_1, v_2) = \frac{c}{(1-v_1^2)(1-v_2^2)} I_{\sigma(\hat{v})}(v_1, v_2), \quad c = \text{const.} \quad (2)$$

where,

$$\sigma(\hat{v}) = \left\{ (v_1, v_2) \mid \frac{(v_1 + v_2)^2}{4a} + \frac{(v_1 - v_2)^2}{4(1-a)} < 1 \right\}. \quad (3)$$

However, these studies did not uncover the relationships between two-dimensional walks and one-dimensional Konno distribution. We obtained a novel two-dimensional probability distribution from which the one-dimensional Konno distribution can be derived by taking a certain type of limit. Our distribution can also reproduce the distribution obtained in [12, 13] under a certain conditions.

We denote the two-dimensional lattice representing positions by  $\mathbb{Z}^2 := \{x = (x_1, x_2) \mid x_1, x_2 \in \mathbb{Z}\}$ . The Hilbert space of states is  $\mathcal{H} := \ell^2(\mathbb{Z}^2; \mathbb{C}^2) \simeq \ell^2(\mathbb{Z}^2) \otimes \mathbb{C}^2$ . We define the two-dimensional two-state alternate coin QW model (2D2SQW) as follows:

$$U := S_2 C_2 S_1 C_1, \quad (4)$$

where  $S_q := L_q \oplus L_q^*$  for  $q = 1, 2$  and  $L_q$  is left/down-shift operator on  $\ell^2(\mathbb{Z}^2; \mathbb{C})$  defined by following operations:

$$\begin{aligned} L_1 \Psi(x_1, x_2) &:= \Psi(x_1 + 1, x_2), \\ L_2 \Psi(x_1, x_2) &:= \Psi(x_1, x_2 + 1). \end{aligned} \quad (5)$$

The coin operators are homogeneous across the entire lattice  $C_q = \bigoplus_{x \in \mathbb{Z}^2} C_{0,q}$  with  $C_{0,q} \in U(2)$  are defined as:

$$C_{0,q} := e^{i\delta_q/2} \begin{pmatrix} a_q & b_q \\ -b_q^* & a_q^* \end{pmatrix}, \quad (6)$$

where  $a_q, b_q \in \mathbb{C}$ ,  $z^*$  denotes the complex conjugate of the complex number  $z$ , and the parameters satisfy the following:

$$a_q = |a_q| e^{i\alpha_q}, \quad b_q = |b_q| e^{i\beta_q} \quad (7)$$

$$|a_q|^2 + |b_q|^2 = 1, \quad (8)$$

$$\alpha_q, \beta_q, \delta_q \in [-\pi, \pi), \quad \det C_{0,q} = e^{i\delta_q}. \quad (9)$$

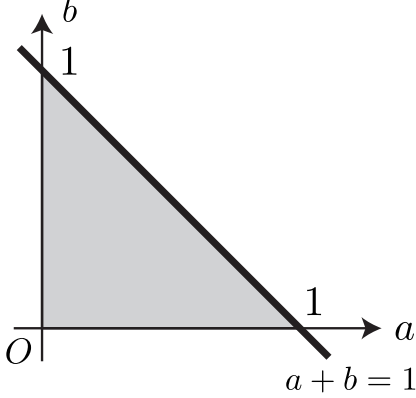
\* keisuke-asahara@biwako.shiga-u.ac.jp

† funakawa@hgu.jp

‡ marmot.motoki@gmail.com

§ akito.suzuki@komatsu-u.ac.jp

FIG. 1. Parameter region for  $(a, b)$ . These parameters can take any value within the interior and on the boundary of this region shaded in gray, except for the boundaries where  $a = 0$  or  $b = 0$ .



We introduce the parameters:

$$a := |a_2||a_1|, \quad b := |b_2||b_1|. \quad (10)$$

From equation (8), these parameters are subject to the constraints  $a + b \leq 1$ ,  $a \geq 0$ , and  $b \geq 0$ . Conversely, the parameters  $(a, b)$  can take any value within this region (FIG. 1). To exclude trivial models, we will disregard cases where the parameters satisfy  $a = 0$  or  $b = 0$ .

The initial state is  $\Psi_0 \in \mathcal{H}$ , and the state at time  $t$  ( $= 0, 1, 2, \dots$ ) is given by  $\Psi_t = U^t \Psi_0$ , where  $\Psi_0$  satisfies the constraint  $\|\Psi_0\| = 1$ . The orthogonal projection operator onto the position  $(x_1, x_2)$  is  $\hat{\Pi}_{(x_1, x_2)}: \mathcal{H} \rightarrow \mathcal{H}$ , defined as

$$(\hat{\Pi}_{(x_1, x_2)} \Psi)(y_1, y_2) := \begin{cases} \Psi(x_1, x_2), & (y_1, y_2) = (x_1, x_2), \\ 0, & \text{otherwise.} \end{cases} \quad (11)$$

The random variables representing the position of the quantum walker in the  $x_1$  and  $x_2$  directions at time  $t$  are denoted by  $X_{1,t}$  and  $X_{2,t}$ , respectively. In this context, the probability that the walker is found at position  $(x_1, x_2)$  when observed at time  $t$  is given by

$$P((X_{1,t}, X_{2,t}) = (x_1, x_2)) = \left\| \hat{\Pi}_{(x_1, x_2)} \Psi_t \right\|^2. \quad (12)$$

When  $a + b = 1$ , the situation is special; therefore, we consider the case  $a + b < 1$  in this paragraph. We have obtained a weak limit theorem using the form of the following characteristic function of  $\xi = (\xi_1, \xi_2) \in \mathbb{R}^2$ :

$$\lim_{t \rightarrow \infty} \mathbb{E} \left( e^{i\xi \cdot X_t/t} \right) = \int_{\sigma(\hat{v})} \frac{dv}{(2\pi)^2} e^{i\xi \cdot v} f(v), \quad (13)$$

where  $\xi \cdot \zeta = \xi_1 \zeta_1 + \xi_2 \zeta_2$  is the scalar product of  $\xi = (\xi_1, \xi_2)$  and  $\zeta = (\zeta_1, \zeta_2)$ . The region  $\sigma(\hat{v})$  of integration is the support of the joint spectral measure  $E_{\hat{v}_1} \otimes E_{\hat{v}_2}$  for the asymptotic velocity operators  $\hat{v}_1$  and  $\hat{v}_2$ , which are defined in the Sec. III A, in the directions of  $x_1$  and  $x_2$ ,

respectively. The support is calculated as the intersection of two ellipses given by

$$\sigma(\hat{v}) = \left\{ (v_1, v_2) \left| \frac{(v_1 + v_2)^2}{-2f_{R,1}(j_+)} + \frac{(v_1 - v_2)^2}{2f_{R,2}(j_+)} \leq 1 \right. \right\} \\ \cap \left\{ (v_1, v_2) \left| \frac{(v_1 + v_2)^2}{2f_{T,1}(j_+)} + \frac{(v_1 - v_2)^2}{-2f_{T,2}(j_+)} \leq 1 \right. \right\} \quad (14)$$

and the constants  $f_{R,1}(j_+)$ ,  $f_{R,2}(j_+)$ ,  $f_{T,1}(j_+)$ , and  $f_{T,2}(j_+)$  are given by:

$$-f_{R,1}(j_+) = 1 + a^2 - b^2 + \sqrt{D_J}, \quad (15)$$

$$f_{R,2}(j_+) = 1 - a^2 + b^2 - \sqrt{D_J}, \quad (16)$$

$$f_{T,1}(j_+) = 1 + a^2 - b^2 - \sqrt{D_J}, \quad (17)$$

$$-f_{T,2}(j_+) = 1 - a^2 + b^2 + \sqrt{D_J}, \quad (18)$$

where  $D_J$  is defined as:

$$D_J := (1 - (a^2 + b^2))^2 - 4a^2b^2 \geq 0. \quad (19)$$

This paper is organized as follows. In Sec. II, we state the main theorem. We prove the main theorem in Sec. III.

## II. MAIN THEOREM

The tuple of variables  $(v_1, v_2)$  is determined by the map  $\mathcal{V} \circ \mathcal{U} \circ \mathcal{C} \circ \mathcal{L}: (k_1, k_2) \mapsto (v_1, v_2)$ , whose concrete definition is given in Sec. III B. As stated in previous section, the case where parameter  $(a, b)$  satisfy  $a + b = 1$  is special. Therefore, we present the theorem separately for the case  $a + b < 1$  and  $a + b = 1$ .

### A. When $a + b < 1$

We denote the absolute Jacobian of the map  $\mathcal{V} \circ \mathcal{U} \circ \mathcal{C} \circ \mathcal{L}$  by  $|J|$ . There are two inverses of the Jacobian, denoted as  $|J|_+^{-1}$  and  $|J|_-^{-1}$ , which are calculated as follows:

$$|J|_{\pm}^{-1} = \frac{B \pm 2ab\sqrt{E_R E_T}}{4ab(1 - v_1^2)(1 - v_2^2)\sqrt{E_R E_T}}, \quad (20)$$

where

$$B = -\frac{1}{2}(v_1^2 + v_2^2) + (a^2 - b^2)v_1 v_2 + 1 - (a^2 + b^2), \quad (21)$$

$$E_R = 1 - \frac{(v_1 + v_2)^2}{-2f_{R,1}(j_+)} - \frac{(v_1 - v_2)^2}{2f_{R,2}(j_+)}, \quad (22)$$

$$E_T = 1 - \frac{(v_1 + v_2)^2}{2f_{T,1}(j_+)} - \frac{(v_1 - v_2)^2}{-2f_{T,2}(j_+)}. \quad (23)$$

Here,  $E_R$  and  $E_T$  are derived from equations of two ellipses. From Eq. (14),  $E_R E_T$  is always positive within the interior of  $\sigma(\hat{v})$ .

**Theorem 1** (Weak limit theorem for 2D2SQW). *When  $a + b < 1$ , Eq. (13) holds and  $f(v)$  is given by*

$$f(v) = |J|_+^{-1} w_+(v) + |J|_-^{-1} w_-(v), \quad (24)$$

where  $w_{\pm}(v)$  are functions of  $v$  determined from Fourier transformed initial state  $\hat{\Psi}_0 = \mathcal{F}\Psi_0$  and eigenvectors of Fourier transformed evolution operator, whose concrete definition is given in Eqs. (103) and (104).

### B. When $a + b = 1$

When  $a + b = 1$ ,  $D_J$  becomes zero, and the inverses of the Jacobian degenerate, as calculated below:

$$|J|^{-1} = \frac{1}{(1 - v_1^2)(1 - v_2^2)}. \quad (25)$$

Furthermore,  $\sigma(\hat{v})$  also degenerates to a single ellipse, which is expressed by the following equation:

$$\sigma(\hat{v}) = \left\{ (v_1, v_2) \left| \frac{(v_1 + v_2)^2}{4a} + \frac{(v_1 - v_2)^2}{4b} \leq 1 \right. \right\}. \quad (26)$$

**Theorem 1'.** *When  $a + b = 1$ , Eq. (13) holds and  $f(v)$  is given by*

$$f(v) = |J|^{-1} w(v) \quad (27)$$

where  $w(v)$  are functions of  $v$  determined from Fourier transformed initial state  $\hat{\Psi}_0 = \mathcal{F}\Psi_0$  and eigenvectors of Fourier transformed evolution operator, whose concrete definition is given in Sec. III.

## III. PROOF

The proof of the main theorem is based on the method by Grimmet *et al.* [4]. We assume  $a + b < 1$  for simplicity from Sec. III A to Sec. III F.

### A. The definition of velocity operator

Let  $\mathbb{T} = [-\pi, \pi)$ . The wavenumber space of the square integrable functions of  $k = (k_1, k_2) \in \mathbb{T}^2$  is

$$\mathcal{K} := L^2\left(\mathbb{T}^2, \frac{dk}{(2\pi)^2}; \mathbb{C}^2\right). \quad (28)$$

Let the Fourier transform operator and its inverse be denoted by  $\mathcal{F}: \mathcal{H} \rightarrow \mathcal{K}$  and  $\mathcal{F}^{-1}: \mathcal{K} \rightarrow \mathcal{H}$ , respectively. The eigenvalues of  $(\mathcal{F}U\mathcal{F}^{-1})(k) \in M_2(\mathbb{C})$  are given by

$$\lambda_p(k) = \left( \tau + (-1)^{p-1} i \sqrt{1 - \tau^2} \right) e^{i\delta/2}, \quad p = 1, 2, \quad (29)$$

where

$$l_1 := k_2 + k_1 + \alpha_2 + \alpha_1, \quad l_2 := k_2 - k_1 + \beta_2 - \beta_1, \quad (30)$$

$$c_1 := \cos l_1, \quad c_2 := \cos l_2, \quad (31)$$

$$s_1 := \sin l_1, \quad s_2 := \sin l_2, \quad (32)$$

$$\tau := ac_1 - bc_2, \quad \delta := \delta_2 + \delta_1. \quad (33)$$

The Fourier transformed time evolution operator is represented by

$$(\mathcal{F}U\mathcal{F}^{-1})(k) = \sum_{p=1,2} \lambda_p(k) |\lambda_p(k)\rangle \langle \lambda_p(k)|, \quad k \in \mathbb{T}^2 \quad (34)$$

where  $|\lambda_p(k)\rangle$  are the eigenvectors corresponding to  $\lambda_p(k)$ . Let

$$v_{p,q}(k) := \frac{i}{\lambda_p(k)} \frac{\partial \lambda_p(k)}{\partial k_q}, \quad p, q = 1, 2. \quad (35)$$

The Hermitian matrices  $\hat{v}_q(k) \in M_2(\mathbb{C})$  are defined by

$$\hat{v}_q(k) := \sum_{p=1,2} v_{p,q}(k) |\lambda_p(k)\rangle \langle \lambda_p(k)|, \quad k \in \mathbb{T}^2. \quad (36)$$

Now, we can define the asymptotic velocity operators  $\hat{v}_q$  so that

$$\mathcal{F} \hat{v}_q \mathcal{F}^{-1} = \int_{\mathbb{T}^2}^{\oplus} \frac{dk}{(2\pi)^2} \hat{v}_q(k), \quad (37)$$

where the integral with the superscripted direct sum represents a direct integral. We denote the tuple of velocity operators by  $\hat{v} = (\hat{v}_1, \hat{v}_2)$ .

Calculating  $v_{p,q}(k)$  from Eqs. (29) and (35), we obtain

$$v_{p,q}(k) = \frac{i}{\lambda_p} \frac{\partial \lambda_p}{\partial k_q} = \frac{(-1)^{p-1}}{\sqrt{1 - \tau^2}} \frac{\partial \tau}{\partial k_q}, \quad (38)$$

where the right hand side is well-defined because  $\tau^2 < 1$  due to  $a + b < 1$ . Explicitly, in terms of  $s_1$  and  $s_2$ , we have

$$\begin{cases} v_{p,1} = (-1)^p \frac{as_1 + bs_2}{\sqrt{1 - \tau^2}}, \\ v_{p,2} = (-1)^p \frac{as_1 - bs_2}{\sqrt{1 - \tau^2}}. \end{cases} \quad (39)$$

The variables  $(v_1, v_2)$  are defined by

$$\begin{cases} v_1 := v_{1,1} = -\frac{as_1 + bs_2}{\sqrt{1 - \tau^2}}, \\ v_2 := v_{1,2} = -\frac{as_1 - bs_2}{\sqrt{1 - \tau^2}}. \end{cases} \quad (40)$$

### B. The region of $\sigma(\hat{v})$

Let the variables  $(u_1, u_2)$  be defined as

$$\begin{pmatrix} u_1 \\ u_2 \end{pmatrix} := \frac{1}{\sqrt{2}} \begin{pmatrix} 1 & 1 \\ 1 & -1 \end{pmatrix} \begin{pmatrix} v_1 \\ v_2 \end{pmatrix}. \quad (41)$$

Explicitly, in terms of  $s_1, s_2, c_1,$  and  $c_2,$  we have

$$\begin{cases} u_1 = -\operatorname{sgn}(s_1)\sqrt{\frac{2a^2(1-c_1^2)}{1-\tau^2}}, \\ u_2 = -\operatorname{sgn}(s_2)\sqrt{\frac{2b^2(1-c_2^2)}{1-\tau^2}}, \end{cases} \quad (42)$$

where  $\operatorname{sgn}(s)$  is sign of  $s$ , that is, 1 if  $s > 0$ , 0 if  $s = 0$ , and  $-1$  if  $s < 0$ .

We define the maps  $\mathcal{L}: (k_1, k_2) \mapsto (l_1, l_2)$  by Eq. (30),  $\mathcal{C}: (l_1, l_2) \mapsto (c_1, c_2)$  by Eq. (31),  $\mathcal{U}: (c_1, c_2) \mapsto (u_1, u_2)$  by Eq. (42), and  $\mathcal{V}: (u_1, u_2) \mapsto (v_1, v_2)$  by Eq. (41) (FIG. 2). Because of the definition of  $\hat{v}_q$  (Eq. (37)), the support  $\sigma(\hat{v})$  of the joint spectral measure  $E_{\hat{v}_1} \otimes E_{\hat{v}_2}$  is calculated from  $\mathcal{V} \circ \mathcal{U} \circ \mathcal{C} \circ \mathcal{L}(\mathbb{T}^2)$ . It is obvious that  $\mathcal{C} \circ \mathcal{L}(\mathbb{T}^2) = [-1, 1]^2$  and  $\mathcal{V}$  is merely linear transform; therefore, the main concern is the calculation of  $\mathcal{U}([-1, 1]^2)$ . Let us divide  $[-1, 1]^2$  into the ribbon like region  $R$  and the twist like region  $T$  defined as (FIG. 3)

$$R := \{(c_1, c_2) \mid c_2 = \kappa c_1, \kappa \in [-1, 1], c_1 \in [-1, 1]\}, \quad (43)$$

$$T := \{(c_1, c_2) \mid c_1 = \gamma c_2, \gamma \in [-1, 1], c_2 \in [-1, 1]\}. \quad (44)$$

**Proposition 2.** *The images  $\mathcal{U}(R)$  and  $\mathcal{U}(T)$  of the regions  $R$  and  $T$  under the map  $\mathcal{U}$  are calculated as follows:*

$$\mathcal{U}(R) = \left\{ (u_1, u_2) \mid \frac{u_1^2}{-f_{R,1}(j_+)} + \frac{u_2^2}{f_{R,2}(j_+)} \leq 1 \right\} \cap \{(u_1, u_2) \mid a|u_2| \geq b|u_1|\}, \quad (45)$$

$$\mathcal{U}(T) = \left\{ (u_1, u_2) \mid \frac{u_1^2}{f_{T,1}(j_+)} + \frac{u_2^2}{-f_{T,2}(j_+)} \leq 1 \right\} \cap \{(u_1, u_2) \mid a|u_2| \leq b|u_1|\}. \quad (46)$$

Moreover, the image  $\mathcal{U}([-1, 1]^2)$  is an union of  $\mathcal{U}(R)$  and  $\mathcal{U}(T)$  with:

$$\begin{aligned} \mathcal{U}([-1, 1]^2) &= \mathcal{U}(R) \cup \mathcal{U}(T) \\ &= \left\{ (u_1, u_2) \mid \frac{u_1^2}{-f_{R,1}(j_+)} + \frac{u_2^2}{f_{R,2}(j_+)} \leq 1 \right\} \\ &\quad \cap \left\{ (u_1, u_2) \mid \frac{u_1^2}{f_{T,1}(j_+)} + \frac{u_2^2}{-f_{T,2}(j_+)} \leq 1 \right\}, \end{aligned} \quad (47)$$

This proposition is proved in Appendix Sec. A.

Calculating  $\mathcal{V} \circ \mathcal{U}([-1, 1]^2)$  from this proposition and Eq. (41), we obtain  $\sigma(\hat{v})$ .

### C. Jacobian

To prove Theorem 1, it is necessary to express the inverse of the Jacobian as a function of the variables  $(v_1, v_2)$ . The absolute Jacobian is calculated as follows:

$$\begin{aligned} |J| &= \left| \det \left( \frac{dv}{dk} \right) \right| \\ &= \frac{4abc_1^2}{(1-\tau^2)^2} \varphi \left( \frac{c_2}{c_1} \right), \end{aligned} \quad (48)$$

where  $\varphi(x)$  is the following quadratic polynomial:

$$\varphi(x) := abx^2 + (1 - (a^2 + b^2))x + ab. \quad (49)$$

The solutions and discriminant of  $\varphi(x) = 0$  are as follows:

$$j_{\pm} := \frac{1}{2ab} \left\{ -(1 - (a^2 + b^2)) \pm \sqrt{D_J} \right\}, \quad (50)$$

$$\begin{aligned} D_J &:= (1 - (a^2 + b^2))^2 - 4a^2b^2 \\ &= (1 - (a + b)^2)(1 - (a - b)^2). \end{aligned} \quad (51)$$

From Eq. (51), we obtain  $D_J \geq 0$  and  $j_- \leq -1 \leq j_+ < 0$  because  $j_- \cdot j_+ = 1$ .

**Theorem 3** (the inverse of absolute Jacobian). *The inverse of absolute Jacobian  $|J|_{\pm}^{-1}$  is given by*

$$|J|_{\pm}^{-1} = \frac{B \pm 2ab\sqrt{E_R E_T}}{4ab(1-v_1^2)(1-v_2^2)\sqrt{E_R E_T}}, \quad (52)$$

where

$$\begin{aligned} B &:= (a^2 - b^2) \left( \frac{u_1^2}{2} - \frac{u_2^2}{2} \right) - \left( \frac{u_1^2}{2} + \frac{u_2^2}{2} \right) \\ &\quad + 1 - (a^2 + b^2), \end{aligned} \quad (53)$$

which can be transformed into Eq. (21) via Eq. (41). Additionally,

$$E_R := 1 - \frac{u_1^2}{-f_{R,1}(j_+)} - \frac{u_2^2}{f_{R,2}(j_+)}, \quad (54)$$

$$E_T := 1 - \frac{u_1^2}{f_{T,1}(j_+)} - \frac{u_2^2}{-f_{T,2}(j_+)}, \quad (55)$$

which can be transformed into Eq. (22) and (23) via Eq. (41).

*Proof.* It is necessary to express  $1 - \tau^2$  in terms of variables  $(u_1, u_2)$ , and consequently in terms of the variables  $(v_1, v_2)$ . From Eq. (33), we obtain the following equation:

$$a^4 c_1^4 + b^4 c_2^4 + \tau^4 - 2a^2 b^2 c_1^2 c_2^2 - 2(a^2 c_1^2 + b^2 c_2^2) \tau^2 = 0. \quad (56)$$

From Eq. (42), we derive the following equations:

$$c_1^2 = 1 - \frac{(1 - \tau^2)u_1^2}{2a^2}, \quad (57)$$

$$c_2^2 = 1 - \frac{(1 - \tau^2)u_2^2}{2b^2}. \quad (58)$$

We then obtain the following expression:

$$\tau^4 = (1 - \tau^2)^2 - 2(1 - \tau^2) + 1. \quad (59)$$

Substituting Eqs. (57), (58), and (59) into Eq. (56), we obtain the following quadratic equation in  $1 - \tau^2$ :

$$A(1 - \tau^2)^2 - 2B(1 - \tau^2) + C = 0, \quad (60)$$

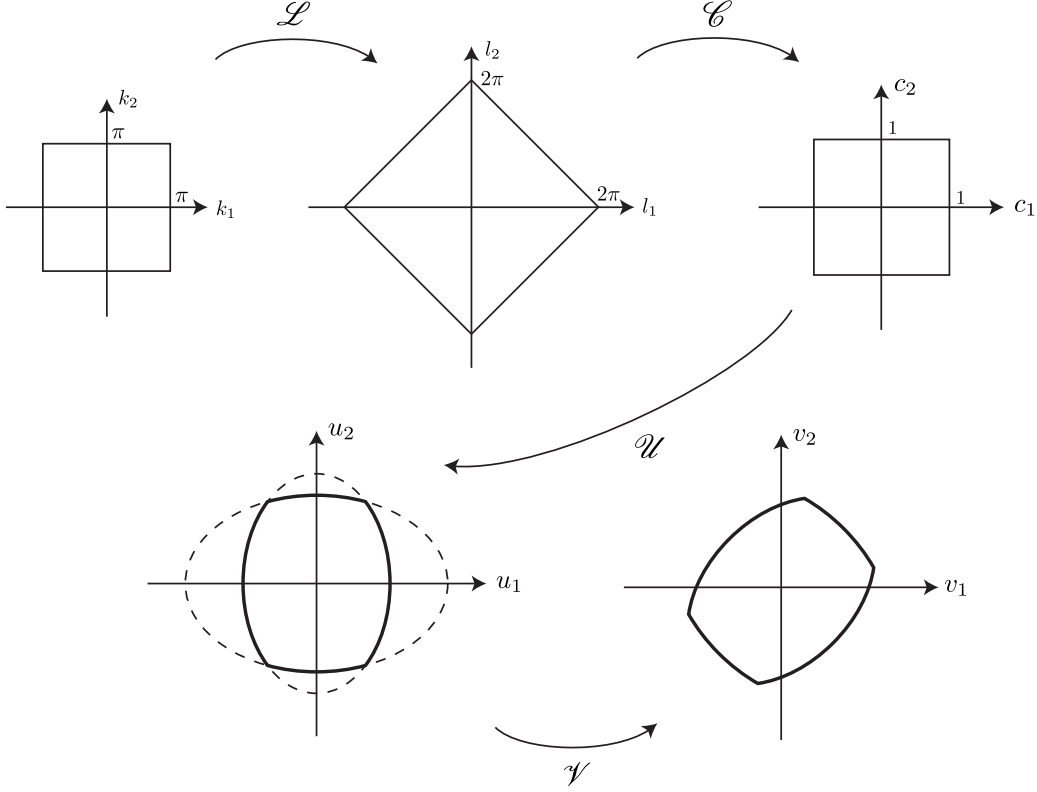
FIG. 2. The images of the maps  $\mathcal{L}$ ,  $\mathcal{C}$ ,  $\mathcal{U}$ , and  $\mathcal{V}$ .

FIG. 3. Division  $[-1, 1]^2$  into  $R$  and  $T$ . The region shaded with red grids in the shape of a ribbon represents  $R$ , while the region shaded with blue diagonal lines in the shape of a twist represents  $T$ .

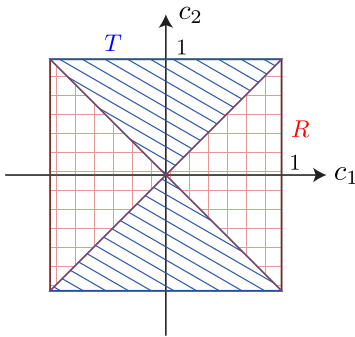
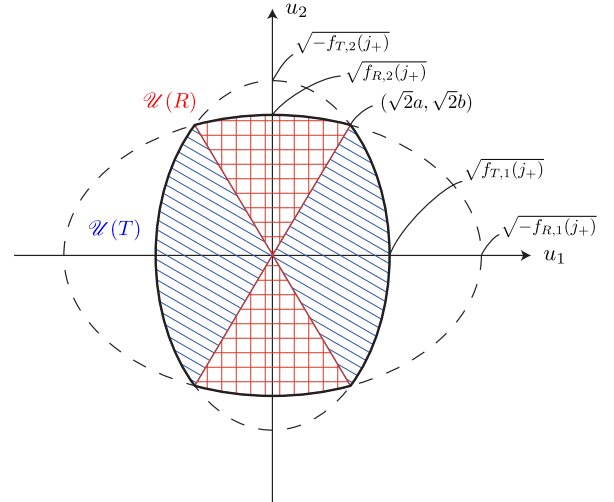


FIG. 4. The image  $\mathcal{U}([-1, 1]^2)$ . The region shaded with red grids represents  $\mathcal{U}(R)$ , while the region shaded with blue diagonal lines represents  $\mathcal{U}(T)$ .



where

$$A := (1 - v_1^2)(1 - v_2^2), \quad (61)$$

$$B := (a^2 - b^2) \left( \frac{u_1^2}{2} - \frac{u_2^2}{2} \right) - \left( \frac{u_1^2}{2} + \frac{u_2^2}{2} \right) + 1 - (a^2 + b^2), \quad (62)$$

$$C := D_J. \quad (63)$$

We denote the discriminant of Eq. (60) as  $D_{1-\tau^2}/4$ , and

calculate it as follows:

$$D_{1-\tau^2}/4 = b^2 u_1^4 + a^2 u_2^4 + (1 - (a^2 + b^2)) u_1^2 u_2^2 - 2b^2(1 + a^2 - b^2) u_1^2 - 2a^2(1 - a^2 + b^2) u_2^2 + 4a^2 b^2. \quad (64)$$

Using this expression, we obtain the solution as follows:

$$1 - \tau^2 = \frac{B \pm \sqrt{D_{1-\tau^2}/4}}{A}. \quad (65)$$

From Eq. (47), we obtain Eqs. (54) and (55), which can be transformed into Eq. (22) and (23) via Eq. (41). We calculate their product as follows:

$$4a^2b^2E_RE_T = D_{1-\tau^2}/4. \quad (66)$$

Moreover, from Eq. (60), we derive the following equation:

$$B(1 - \tau^2) - C = A(1 - \tau^2)^2 - B(1 - \tau^2). \quad (67)$$

From Eq. (33), we obtain the following expression:

$$c_1c_2 = \frac{a^2c_1^2 + b^2c_2^2 - \tau^2}{2ab}. \quad (68)$$

Substituting Eqs. (57), (58), (67), and (68) into Eq. (48), we derive the following equation:

$$|J| = \frac{2\sqrt{D_{1-\tau^2}/4}}{1 - \tau^2}. \quad (69)$$

Therefore, from Eqs. (65) and (66), the inverse of the absolute Jacobian is obtained as Eq. (52). Finally, we obtain Eq. (20).  $\square$

Up to this point, we have demonstrated the expression for  $|J|_{\pm}^{-1}$  in Eq. (24). However, we will now discuss how the sign is selected and how to calculate  $w_{\pm}(v)$ .

#### D. Bijectivity of the maps

Since constructing the inverse map is necessary, the map  $\mathcal{V} \circ \mathcal{U} \circ \mathcal{C} \circ \mathcal{L}$  must be bijective for the proof of the main theorem later. To begin with, we analyze the map  $\mathcal{L}$  in detail. For simplicity, we assume  $\alpha_q, \beta_q = 0$  in Eq. (7) for  $q = 1, 2$ , and will consider the effect later. Hence, the map  $\mathcal{L}$  becomes linear and can be written as follows:

$$\begin{pmatrix} l_1 \\ l_2 \end{pmatrix} = \mathcal{L} \begin{pmatrix} k_1 \\ k_2 \end{pmatrix} = \begin{pmatrix} 1 & 1 \\ -1 & 1 \end{pmatrix} \begin{pmatrix} k_1 \\ k_2 \end{pmatrix}. \quad (70)$$

Because  $(k_1, k_2) \in \mathbb{T}^2$  and the integrand have a periodic boundary condition, we transform  $\mathbb{T}^2$  into the region shaped like a windmill as shown in FIG. 5. Furthermore, we divide the windmill region into eight square regions and label them from  $K_1$  to  $K_8$ . From the linearity of  $\mathcal{L}$ , the following proposition holds.

**Proposition 4.** *The square regions, from  $K_1$  to  $K_8$ , are bijectively mapped by  $\mathcal{L}$  to  $L_1$  through  $L_8$ .*

Note that the signs  $-\text{sgn}(s_1)$  and  $-\text{sgn}(s_2)$  in Eq. (42) are constant in the interior of each region  $L_n$  ( $n = 1, \dots, 8$ ) (TABLE I).

Turning the discussion to the map  $\mathcal{C}$ , the following proposition is obvious.

TABLE I. A correspondence table between the region  $L_n$  in the  $l_1l_2$ -plane and the quadrants in the  $u_1u_2$ -plane.

$n$	$-\text{sgn}(s_1)$	$-\text{sgn}(s_2)$	quadrant
1	–	–	3
2	+	–	4
3	+	+	1
4	–	+	2
5	–	–	3
6	+	–	4
7	+	+	1
8	–	+	2

**Proposition 5.** *Each square region  $L_n$  is mapped by  $\mathcal{C}$  to  $[-1, 1]^2$  on  $c_1c_2$ -plane bijectively.*

In particular, the map  $\mathcal{U}$  is complicated because Eq. (42) is. The region  $[-1, 1]^2$  on the  $c_1c_2$ -plane is divided into four regions by the lines  $c_2 = j_+c_1$  and  $c_1 = j_+c_2$ , and labeled from  $C_1$  to  $C_4$  as follows:

$$C_1 := \{(c_1, c_2) \mid c_1 \leq j_+c_2, c_2 \geq j_+c_1\} \cap [-1, 1]^2, \quad (71)$$

$$C_2 := \{(c_1, c_2) \mid c_1 \leq j_+c_2, c_2 \leq j_+c_1\} \cap [-1, 1]^2, \quad (72)$$

$$C_3 := \{(c_1, c_2) \mid c_1 \geq j_+c_2, c_2 \leq j_+c_1\} \cap [-1, 1]^2, \quad (73)$$

$$C_4 := \{(c_1, c_2) \mid c_1 \geq j_+c_2, c_2 \geq j_+c_1\} \cap [-1, 1]^2. \quad (74)$$

When  $\mathcal{C}(L_n)$  is mapped by  $\mathcal{U}$ , its image is confined to the  $(n + 2) \bmod 4$ -th quadrant according to Eq. (42), where the 0-th quadrant should be interpreted as the 4-th quadrant.

**Proposition 6.** *For the map  $\mathcal{U}$ , if the domain is restricted to  $\mathcal{C}(L_n) \cap C_m$  ( $m = 1, \dots, 4$ ) and the image is restricted to the  $(n + 2) \bmod 4$ -th quadrant of the  $u_1u_2$ -plane, then the map  $\mathcal{U}$  becomes bijective.*

This proposition is proved in Appendix Sec. B.

**Proposition 7.** *The map  $\mathcal{V}$  is obviously bijective because it is linear.*

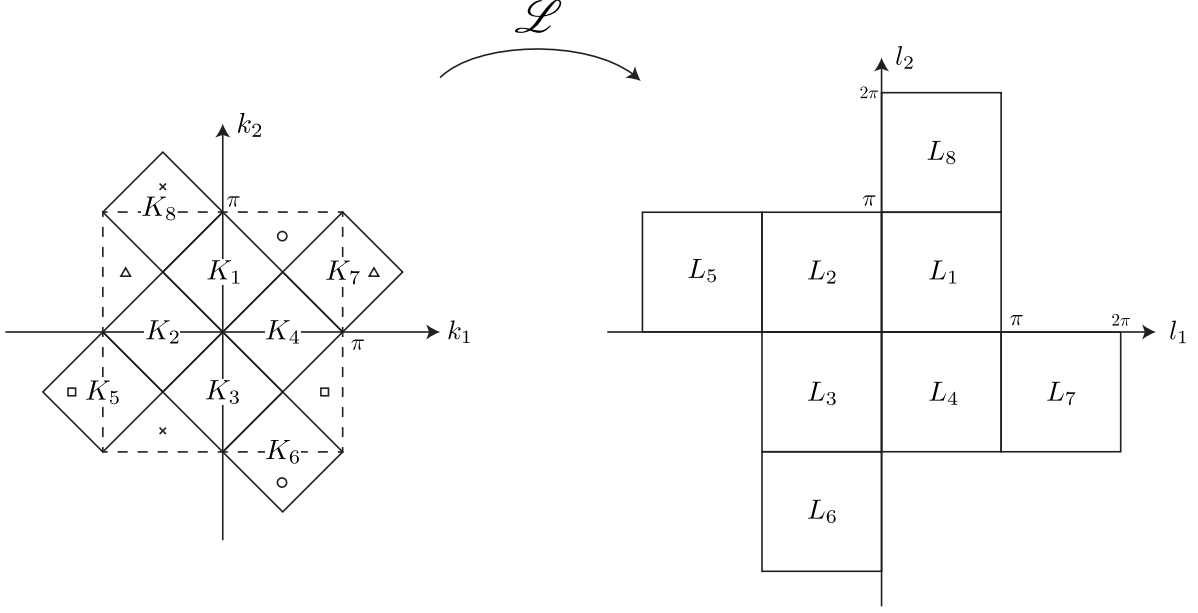
#### E. The sign of $\kappa_{\pm}/\gamma_{\pm}$ and $|J|_{\pm}^{-1}$

**Proposition 8.** *The maps  $(u_1, u_2) \mapsto \kappa$  and  $(u_1, u_2) \mapsto \gamma$  have their respective domains  $\mathcal{U}(R)$  and  $\mathcal{U}(T)$ , and are given by the following:*

$$\kappa_{\pm}(u_1, u_2) = \frac{a b^2 u_1^2 - a^2 u_2^2 \pm \sqrt{D_{1-\tau^2}/4}}{b \ 2a^2 - (1 - b^2)u_1^2 - a^2 u_2^2}, \quad (75)$$

$$\gamma_{\pm}(u_1, u_2) = \frac{b b^2 u_1^2 - a^2 u_2^2 \pm \sqrt{D_{1-\tau^2}/4}}{a \ -2b^2 + b^2 u_1^2 + (1 - a^2)u_2^2}. \quad (76)$$

The signs of  $\kappa_{\pm}$ ,  $\gamma_{\pm}$ , and  $|J|_{\pm}^{-1}$  are determined by the index  $m$  of  $C_m$ ; when  $m$  is odd, the negative sign chosen, and when  $m$  is even, the positive sign chosen as shown in TABLE II.

FIG. 5. Transformation from  $\mathbb{T}^2$  into the windmill region.TABLE II. The signs of  $\kappa_{\pm}/\gamma_{\pm}$  and  $|J|_{\pm}^{-1}$ .

$m$	$R/T$	$\kappa_{\pm}/\gamma_{\pm}$	$ J _{\pm}^{-1}$
1	$R$	$\kappa_-$	$ J _-^{-1}$
1	$T$	$\gamma_-$	$ J _-^{-1}$
2	$R$	$\kappa_+$	$ J _+^{-1}$
2	$T$	$\gamma_+$	$ J _+^{-1}$
3	$R$	$\kappa_-$	$ J _-^{-1}$
3	$T$	$\gamma_-$	$ J _-^{-1}$
4	$R$	$\kappa_+$	$ J _+^{-1}$
4	$T$	$\gamma_+$	$ J _+^{-1}$

### F. Proof of the main theorem

We define the orthogonal projection operator for the position  $x_q$  in the  $q$  direction for  $q = 1, 2$  as follows:

$$\hat{\Pi}_{1,x_1} := \sum_{x_2 \in \mathbb{Z}} \hat{\Pi}_{(x_1, x_2)}, \quad (77)$$

$$\hat{\Pi}_{2,x_2} := \sum_{x_1 \in \mathbb{Z}} \hat{\Pi}_{(x_1, x_2)}. \quad (78)$$

Since these are bounded self-adjoint operators, they commute as follows:

$$\hat{\Pi}_{(x_1, x_2)} = \hat{\Pi}_{1,x_1} \hat{\Pi}_{2,x_2} = \hat{\Pi}_{2,x_2} \hat{\Pi}_{1,x_1}. \quad (79)$$

Using these operators, the position operators  $\hat{x}_q: \mathcal{H} \rightarrow \mathcal{H}$  in the  $q$  directions are defined as follows:

$$\hat{x}_q := \sum_{x \in \mathbb{Z}} x \hat{\Pi}_{q,x}, \quad (80)$$

which satisfy

$$(\hat{x}_q \Psi)(x_1, x_2) = x_q \Psi(x_1, x_2), \quad (x_1, x_2) \in \mathbb{Z}^2, \Psi \in \mathcal{H}. \quad (81)$$

Furthermore, we define the Heisenberg operators  $\hat{x}_q(t): \mathcal{H} \rightarrow \mathcal{H}$  as follows:

$$\hat{x}_q(t) := U^{-t} \hat{x}_q U^t. \quad (82)$$

**Lemma 9.** *The characteristic function of  $X_t/t := (X_{1,t}/t, X_{2,t}/t)$  is given by*

$$\mathbb{E}\left(e^{i\xi \cdot X_t/t}\right) = \left\langle \Psi_0 \left| e^{i\xi \cdot \hat{x}(t)/t} \right| \Psi_0 \right\rangle, \quad \xi := (\xi_1, \xi_2) \in \mathbb{R}^2. \quad (83)$$

*Proof.* The distribution of  $X_t$  is expressed as follows:

$$P((X_{1,t}, X_{2,t}) = (x_1, x_2)) = \left\langle \Psi_0 \left| U^{-t} \hat{\Pi}_{(x_1, x_2)} U^t \right| \Psi_0 \right\rangle. \quad (84)$$

From the definition of the characteristic function of  $X_t/t$ , we calculate as follows:

$$\begin{aligned} \mathbb{E}\left(e^{i\xi X_t/t}\right) &= \sum_{(x_1, x_2) \in \mathbb{Z}^2} e^{i(\xi_1 x_1/t + \xi_2 x_2/t)} P((X_{1,t}, X_{2,t}) = (x_1, x_2)) \\ &= \left\langle \Psi_0 \left| U^{-t} \left( \sum_{(x_1, x_2) \in \mathbb{Z}^2} e^{i(\xi_1 x_1/t + \xi_2 x_2/t)} \hat{\Pi}_{(x_1, x_2)} \right) U^t \right| \Psi_0 \right\rangle \\ &= \left\langle \Psi_0 \left| e^{i\xi \cdot \hat{x}(t)/t} \right| \Psi_0 \right\rangle \end{aligned} \quad (85)$$

Therefore, Eq. (83) holds.  $\square$

We introduce the following theorem which is proved almost in parallel with the proof in the Section 4.1 of [5].

**Theorem 10.** *We suppose  $\hat{x}_q(t)$  and  $\hat{v}_q$  are defined in Eqs. (82) and (37), respectively. We assume the function  $(k_1, k_2) \mapsto |\lambda_p(k_1, k_2)\rangle$  are continuously differentiable in  $(k_1, k_2)$  with*

$$\sup_{k \in \mathbb{T}^2} \left\| \frac{\partial}{\partial k_q} |\lambda_p(k)\rangle \right\|_{\mathbb{C}^2} < \infty. \quad (86)$$

Then,

$$\text{s-lim}_{t \rightarrow \infty} \exp\left(i\xi_q \frac{\hat{x}_q(t)}{t}\right) = \exp(i\xi_q \hat{v}_q), \quad \xi_q \in \mathbb{R}. \quad (87)$$

*Proof of Theorem 1.* From Lemma 9 and Theorem 10, we

proceed as follows:

$$\begin{aligned} & \lim_{t \rightarrow \infty} \mathbb{E}\left(e^{i\xi \cdot X_t/t}\right) \\ &= \langle \Psi_0 | e^{i\xi \cdot \hat{v}} | \Psi_0 \rangle \\ &= \langle \hat{\Psi}_0 | e^{i\xi \cdot \mathcal{F} \hat{v} \mathcal{F}^{-1}} | \hat{\Psi}_0 \rangle \\ &= \int_{\mathbb{T}^2} \frac{dk}{(2\pi)^2} \sum_{p=1,2} e^{i \sum_{q=1,2} \xi_q v_{p,q}(k)} \left| \langle \hat{\Psi}_0 | \lambda_p(k) \rangle \right|^2. \end{aligned} \quad (88)$$

We denote by  $P_p(k) = \left| \langle \hat{\Psi}_0 | \lambda_p(k) \rangle \right|^2$ . Let us recall  $\alpha_q, \beta_q$  for  $q = 1, 2$  in Eq. (7). If these parameters are not zero, the region  $L_n$  in the  $l_1 l_2$ -plane will deviate from the configuration shown in the FIG. 5, causing the subsequent argument to collapse. Therefore, we consider the following transformation:

$$k'_1 := k_1 - \phi_1, \quad (89)$$

$$k'_2 := k_2 - \phi_2, \quad (90)$$

where

$$\phi_1 := \frac{1}{2}(\alpha_2 + \alpha_1 - \beta_2 + \beta_1), \quad (91)$$

$$\phi_2 := \frac{1}{2}(\alpha_2 + \alpha_1 + \beta_2 - \beta_1). \quad (92)$$

Applying this transformation, the following relation holds:

$$\mathcal{L} \begin{pmatrix} k_1 \\ k_2 \end{pmatrix} = \begin{pmatrix} 1 & 1 \\ -1 & 1 \end{pmatrix} \begin{pmatrix} k'_1 \\ k'_2 \end{pmatrix}. \quad (93)$$

By applying this transformation, the effects of  $\alpha_q$  and  $\beta_q$  can be canceled out, and from Proposition 4, Eq. (88) can be rewritten as follows:

$$\begin{aligned} \lim_{t \rightarrow \infty} \mathbb{E}\left(e^{i\xi \cdot X_t/t}\right) &= \int_{-\pi}^{\pi} \frac{dk_1}{2\pi} \int_{-\pi}^{\pi} \frac{dk_2}{2\pi} \sum_{p=1,2} e^{i(\xi_1 v_{p,1}(k_1, k_2) + \xi_2 v_{p,2}(k_1, k_2))} P_p(k_1, k_2) \\ &= \int_{-\pi}^{\pi} \frac{dk'_1}{2\pi} \int_{-\pi}^{\pi} \frac{dk'_2}{2\pi} \sum_{p=1,2} e^{i(\xi_1 v_{p,1}(k'_1 + \phi_1, k'_2 + \phi_2) + \xi_2 v_{p,2}(k'_1 + \phi_1, k'_2 + \phi_2))} P_p(k'_1 + \phi_1, k'_2 + \phi_2) \\ &= \sum_{n=1}^8 \int_{L_n} \frac{dl_1 dl_2}{2(2\pi)^2} \sum_{p=1,2} e^{i \sum_{q=1,2} \xi_q v_{p,q}(k_1(l_1, l_2), k_2(l_1, l_2))} P_p(k_1(l_1, l_2), k_2(l_1, l_2)). \end{aligned} \quad (94)$$

By performing a change of variables using the mapping  $\mathcal{C}$  in Eq. (94), and further applying equations (71)–(74),

we obtain the following:

$$\begin{aligned} & (94) \\ &= \sum_{n=1}^8 \int_{\mathcal{C}(L_n)} \frac{dc}{(2\pi)^2} \left| \frac{dc}{dk} \right| \sum_{p=1,2} e^{i \sum_{q=1,2} \xi_q v_{p,q}(k(c))} P_p(k(c)) \\ &= \sum_{n=1}^8 \sum_{m=1}^4 \int_{C_m} \frac{dc}{(2\pi)^2} \left| \frac{dc}{dk} \right| \\ & \quad \times \sum_{p=1,2} e^{i \sum_{q=1,2} \xi_q v_{p,q}(k(c))} P_p(k(c)). \end{aligned} \quad (95)$$



Here,  $|dc/dk|$  and  $k(c)$  are expected to depend on  $n$ , but since we will discuss this dependency later, we do not explicitly write here.

$$\begin{aligned}
(95) &= \sum_{n=1}^8 \sum_{m=1}^4 \int_{\mathcal{W}(C_m)_{(n+2)}} \frac{du}{(2\pi)^2} \left| \frac{du}{dk} \right| \\
&\quad \times \sum_{p=1,2} e^{i \sum_{q=1,2} \xi_q v_{p,q}(k(u))} P_p(k(u)) \\
&= \sum_{n=1}^8 \sum_{m=1}^4 \int_{\mathcal{V} \circ \mathcal{W}(C_m)_{(n+2)}} \frac{dv}{(2\pi)^2} |J|_{(-1)^m}^{-1} \\
&\quad \times \sum_{p=1,2} e^{i \sum_{q=1,2} \xi_q v_{p,q}(k(v))} P_p(k(v)) \quad (96)
\end{aligned}$$

Here, the  $(n+2)$  of the integration region signifies that the integration region is restricted to the  $(n+2) \bmod 4$ -th quadrant of the  $u_1 u_2$ -plane. Note that in the rightmost term, the restricted region is mapped by the transformation  $\mathcal{V}$ , making it the new integration region. Following this,  $v_{p,q}(k(v))$  becomes equal to the variable  $v_{p,q}$ . By utilizing the fact that  $v_{2,q} = -v_{1,q} = -v_q$ , if we change the variable to  $v_q$ , then  $dv_{p=2} = dv_{p=1}$ . Since  $|J|^{-1}$  and  $P_p(k(v))$  are even functions with respect to  $v_q$ , they remain unaffected by this change of variables, and extract-

ing and calculating a part of Eq. (96) gives:

$$\begin{aligned}
&\int_{\mathcal{V} \circ \mathcal{W}(C_m)_{(n+2)}} \frac{dv}{(2\pi)^2} |J|_{(-1)^m}^{-1} e^{i \sum_{q=1,2} \xi_q v_{2,q}(k(v))} P_2(k(v)) \\
&= \int_{\mathcal{V} \circ \mathcal{W}(C_m)_{(n+2)}} \frac{dv}{(2\pi)^2} |J|_{(-1)^m}^{-1} e^{-i \sum_q \xi_q v_{1,q}} P_2(k(v)) \\
&= \int_{\mathcal{V} \circ \mathcal{W}(C_m)_{(n)}} \frac{dv}{(2\pi)^2} |J|_{(-1)^m}^{-1} e^{i \xi \cdot v} P_2(k(v)). \quad (97)
\end{aligned}$$

The sets  $S_1, \dots, S_4$  on the  $v_1 v_2$ -plane are defined as follows:

$$S_1 := \{(v_1, v_2) \mid |v_1| \leq |v_2|, v_1 \geq 0\} \cap \sigma(\hat{v}), \quad (98)$$

$$S_2 := \{(v_1, v_2) \mid |v_1| \geq |v_2|, v_2 \geq 0\} \cap \sigma(\hat{v}), \quad (99)$$

$$S_3 := \{(v_1, v_2) \mid |v_1| \leq |v_2|, v_1 \leq 0\} \cap \sigma(\hat{v}), \quad (100)$$

$$S_4 := \{(v_1, v_2) \mid |v_1| \geq |v_2|, v_2 \leq 0\} \cap \sigma(\hat{v}), \quad (101)$$

Using the result of Eq. (97) and the sets  $S_1, \dots, S_4$ , Eq. (96) can be expressed as follows:

$$\begin{aligned}
(96) &= \int_{S_3} \frac{dv}{(2\pi)^2} |J|_{-}^{-1} e^{i \xi \cdot v} P_1(k(v)) \\
&\quad + \int_{S_1} \frac{dv}{(2\pi)^2} |J|_{-}^{-1} e^{i \xi \cdot v} P_2(k(v)) \\
&\quad + \dots \\
&\quad + \int_{S_2} \frac{dv}{(2\pi)^2} |J|_{+}^{-1} e^{i \xi \cdot v} P_1(k(v)) \\
&\quad + \int_{S_4} \frac{dv}{(2\pi)^2} |J|_{+}^{-1} e^{i \xi \cdot v} P_2(k(v)) \\
&= \int_{\sigma(\hat{v})} \frac{dv}{(2\pi)^2} e^{i \xi \cdot v} \{ |J|_{+}^{-1} w_+(v) + |J|_{-}^{-1} w_-(v) \}, \quad (102)
\end{aligned}$$

where

$$w_+(v) = \begin{cases} \sum_{n'=1}^2 \sum_{m'=1}^2 P_1 \left( k(v) \left| \begin{array}{l} n=4n'-1 \\ m=2m' \\ s=R, T \end{array} \right. \right) + \sum_{n'=1}^2 \sum_{m'=1}^2 P_2 \left( k(v) \left| \begin{array}{l} n=4n'-3 \\ m=2m' \\ s=R, T \end{array} \right. \right), & v \in S_1, \\ \sum_{n'=1}^2 \sum_{m'=1}^2 P_1 \left( k(v) \left| \begin{array}{l} n=4n' \\ m=2m' \\ s=R, T \end{array} \right. \right) + \sum_{n'=1}^2 \sum_{m'=1}^2 P_2 \left( k(v) \left| \begin{array}{l} n=4n'-2 \\ m=2m' \\ s=R, T \end{array} \right. \right), & v \in S_2, \\ \sum_{n'=1}^2 \sum_{m'=1}^2 P_1 \left( k(v) \left| \begin{array}{l} n=4n'-3 \\ m=2m' \\ s=R, T \end{array} \right. \right) + \sum_{n'=1}^2 \sum_{m'=1}^2 P_2 \left( k(v) \left| \begin{array}{l} n=4n'-1 \\ m=2m' \\ s=R, T \end{array} \right. \right), & v \in S_3, \\ \sum_{n'=1}^2 \sum_{m'=1}^2 P_1 \left( k(v) \left| \begin{array}{l} n=4n'-2 \\ m=2m' \\ s=R, T \end{array} \right. \right) + \sum_{n'=1}^2 \sum_{m'=1}^2 P_2 \left( k(v) \left| \begin{array}{l} n=4n' \\ m=2m' \\ s=R, T \end{array} \right. \right), & v \in S_4, \end{cases} \quad (103)$$

$$w_-(v) = \begin{cases} \sum_{n'=1}^2 \sum_{m'=1}^2 P_1 \left( k(v) \left| \begin{array}{l} n=4n'-1 \\ m=2m'-1 \end{array} \right. \right) + \sum_{n'=1}^2 \sum_{m'=1}^2 P_2 \left( k(v) \left| \begin{array}{l} n=4n'-3 \\ m=2m'-1 \end{array} \right. \right), & v \in S_1, \\ \sum_{n'=1}^2 \sum_{m'=1}^2 P_1 \left( k(v) \left| \begin{array}{l} n=4n' \\ m=2m'-1 \end{array} \right. \right) + \sum_{n'=1}^2 \sum_{m'=1}^2 P_2 \left( k(v) \left| \begin{array}{l} n=4n'-2 \\ m=2m'-1 \end{array} \right. \right), & v \in S_2, \\ \sum_{n'=1}^2 \sum_{m'=1}^2 P_1 \left( k(v) \left| \begin{array}{l} n=4n'-3 \\ m=2m'-1 \end{array} \right. \right) + \sum_{n'=1}^2 \sum_{m'=1}^2 P_2 \left( k(v) \left| \begin{array}{l} n=4n'-1 \\ m=2m'-1 \end{array} \right. \right), & v \in S_3, \\ \sum_{n'=1}^2 \sum_{m'=1}^2 P_1 \left( k(v) \left| \begin{array}{l} n=4n'-2 \\ m=2m'-1 \end{array} \right. \right) + \sum_{n'=1}^2 \sum_{m'=1}^2 P_2 \left( k(v) \left| \begin{array}{l} n=4n' \\ m=2m'-1 \end{array} \right. \right), & v \in S_4. \end{cases} \quad (104)$$

Therefore, the theorem holds.  $\square$

The map  $k(v) = (\mathcal{L}^{-1} \circ \mathcal{C}^{-1} \circ \mathcal{U}^{-1} \circ \mathcal{V}^{-1})(v)$  needs to be defined to ensure it is a bijection. The function  $k(v)$  depends on the indices  $p, n, m$  and the shape  $s = R, T$ , the details of which will be discussed in the following subsection.

### G. How to calculate the inverse maps

To construct the mapping  $k(v)$  as a bijection, we decompose it into individual mappings. First, with respect to  $\mathcal{V}^{-1}$ , Eq. (41) serves as the defining equation for the map  $\mathcal{V}^{-1}$ . Next, for  $\mathcal{U}^{-1}$ , by separating  $u_q$  into its sign and absolute value, we obtain the following:

$$c_1(u_1, u_2) = \text{sgn}(c_1)(u_1, u_2) \times |c_1|(u_1, u_2), \quad (105)$$

$$c_2(u_1, u_2) = \text{sgn}(c_2)(u_1, u_2) \times |c_2|(u_1, u_2). \quad (106)$$

The absolute values are determined from Eqs. (57), (58), and (65). The signs depend on the indices  $m$  and  $s$ , and the specific expressions are provided in TABLE III. Here,  $\text{sgn}(\kappa_+)$  and  $\text{sgn}(\gamma_+)$  are expressed in terms of  $u_1$  and  $u_2$  as follows:

$$\text{sgn}(\kappa_+) = \text{sgn}(-2b^2 + b^2u_1^2 + (1 - a^2)u_2^2), \quad (107)$$

$$\text{sgn}(\gamma_+) = \text{sgn}(2a^2 - (1 - b^2)u_1^2 - a^2u_2^2). \quad (108)$$

The map  $\mathcal{C}^{-1}$  depends on the index  $n$  and is given in TABLE IV.

TABLE III. The signs of  $c_1$  and  $c_2$

$m$	$s$	$\text{sgn}(c_1)$	$\text{sgn}(c_2)$
1	$R$	-1	+1
1	$T$	-1	+1
2	$R$	-1	$-\text{sgn}(\kappa_+)$
2	$T$	$-\text{sgn}(\gamma_+)$	-1
3	$R$	+1	-1
3	$T$	+1	-1
4	$R$	+1	$\text{sgn}(\kappa_+)$
4	$T$	$\text{sgn}(\gamma_+)$	+1

Since the map  $\mathcal{L}$  is a composition of a linear transformation and a translation, constructing its inverse map  $\mathcal{L}^{-1}$  is straightforward.

By combining the above,  $k(v) = (\mathcal{L}^{-1} \circ \mathcal{C}^{-1} \circ \mathcal{U}^{-1} \circ \mathcal{V}^{-1})(v)$  can be constructed.

### Appendix A: The image under the map $\mathcal{U}$

Let us calculate  $\mathcal{U}(R)$ . We apply  $\mathcal{U}$  to the line segment  $c_2 = \kappa c_1$ ,  $c_1 \in [-1, 1]$ . Substituting  $c_2 = \kappa c_1$  into

TABLE IV. The map  $\mathcal{C}^{-1}$ 

$n$	$\begin{pmatrix} l_1 \\ l_2 \end{pmatrix} = \mathcal{C}^{-1} \begin{pmatrix} c_1 \\ c_2 \end{pmatrix}$
1	$\begin{pmatrix} l_1 \\ l_2 \end{pmatrix} = \begin{pmatrix} \text{Arccos } c_1 \\ \text{Arccos } c_2 \end{pmatrix}$
2	$\begin{pmatrix} l_1 \\ l_2 \end{pmatrix} = \begin{pmatrix} -\text{Arccos } c_1 \\ \text{Arccos } c_2 \end{pmatrix}$
3	$\begin{pmatrix} l_1 \\ l_2 \end{pmatrix} = \begin{pmatrix} -\text{Arccos } c_1 \\ -\text{Arccos } c_2 \end{pmatrix}$
4	$\begin{pmatrix} l_1 \\ l_2 \end{pmatrix} = \begin{pmatrix} \text{Arccos } c_1 \\ -\text{Arccos } c_2 \end{pmatrix}$
5	$\begin{pmatrix} l_1 \\ l_2 \end{pmatrix} = \begin{pmatrix} \text{Arccos } c_1 - 2\pi \\ \text{Arccos } c_2 \end{pmatrix}$
6	$\begin{pmatrix} l_1 \\ l_2 \end{pmatrix} = \begin{pmatrix} -\text{Arccos } c_1 \\ \text{Arccos } c_2 - 2\pi \end{pmatrix}$
7	$\begin{pmatrix} l_1 \\ l_2 \end{pmatrix} = \begin{pmatrix} -\text{Arccos } c_1 + 2\pi \\ -\text{Arccos } c_2 \end{pmatrix}$
8	$\begin{pmatrix} l_1 \\ l_2 \end{pmatrix} = \begin{pmatrix} \text{Arccos } c_1 \\ -\text{Arccos } c_2 + 2\pi \end{pmatrix}$

Eq. (42) yields the following:

$$\begin{cases} u_1^2 = \frac{2a^2(1-c_1^2)}{1-(a-b\kappa)^2c_1^2}, \\ u_2^2 = \frac{2b^2(1-\kappa^2c_1^2)}{1-(a-b\kappa)^2c_1^2}. \end{cases} \quad (\text{A1})$$

By combining the two equations, we obtain the following:

$$-b^2\{\kappa^2-(a-b\kappa)^2\}u_1^2+a^2\{1-(a-b\kappa)^2\}u_2^2=2a^2b^2(1-\kappa^2). \quad (\text{A2})$$

Here, we define the functions of  $\kappa$  as follows:

$$f_{R,1}(\kappa) := \frac{2a^2(1-\kappa^2)}{\kappa^2-(a-b\kappa)^2}, \quad (\text{A3})$$

$$f_{R,2}(\kappa) := \frac{2b^2(1-\kappa^2)}{1-(a-b\kappa)^2}, \quad (\text{A4})$$

where  $f_{R,2}(\kappa) \geq 0$  for all  $\kappa \in [-1, 1]$ . In this case, since  $f_{R,1}(\kappa) < 0$  and  $f_{R,2}(\kappa) > 0$ , it follows that

$$\frac{u_1^2}{-f_{R,1}(\kappa)} + \frac{u_2^2}{f_{R,2}(\kappa)} = 1, \quad (\text{A5})$$

implying that the line segment is mapped by  $\mathcal{U}$  to a part of an ellipse. Similarly, since  $f_{R,1}(\kappa) > 0$  and  $f_{R,2}(\kappa) > 0$ , it follows that

$$\frac{u_1^2}{f_{R,1}(\kappa)} - \frac{u_2^2}{f_{R,2}(\kappa)} = -1, \quad (\text{A6})$$

implying that the line segment is mapped by  $\mathcal{U}$  to a part of a hyperbola.

Now, we analyze  $f_{R,1}(\kappa)$  and  $f_{R,2}(\kappa)$ . Both equations have the same domain,  $\kappa \in [-1, 1]$ . The denominator of  $f_{R,1}(\kappa)$  becomes zero when  $\kappa = a/(1+b)$  or  $\kappa = -a/(1-b)$ , and these values satisfy

$$-1 \leq -\frac{a}{1-b} \leq 0 \leq \frac{a}{1+b} \leq 1. \quad (\text{A7})$$

The denominator of  $f_{R,2}(\kappa)$  becomes zero when  $\kappa = (1+a)/b$  or  $\kappa = -(1-a)/b$ , but these values satisfy the following inequalities:

$$-\frac{1-a}{b} \leq -1 < 1 \leq \frac{1+a}{b}. \quad (\text{A8})$$

Moreover, both functions  $f_{R,1}$  and  $f_{R,2}$  attain their local maximum at  $\kappa = j_+$ . Thus, the graphs of  $f_{R,1}(\kappa)$  and  $f_{R,2}(\kappa)$  are shown in FIG. 6. Differentiating  $u_1(c_1, \kappa c_1)$  with respect to  $c_1$ , we obtain

$$\frac{du_1}{dc_1}(c_1, \kappa c_1) = -\sqrt{2}ac_1 \frac{1-(a-b\kappa)^2}{(1-(a-b\kappa)^2c_1^2)^{3/2}} \begin{cases} < 0, & (c_1 > 0), \\ = 0, & (c_1 = 0), \\ > 0, & (c_1 < 0). \end{cases} \quad (\text{A9})$$

Therefore, the line segment  $c_2 = \kappa c_1$ ,  $c_1 \in [-1, 1]$  in the region  $R$  is mapped to the following:

- a part of the line segment

$$u_2 = \pm \frac{b}{a} u_1 \quad (\text{A10})$$

when  $\kappa = \pm 1$ ,

- a part of the hyperbola given by Eq. (A6) when  $\kappa \in (-1, -a/(1-b)) \cup (a/(1+b), 1)$ ,

- a part of the line segment

$$u_2 = \pm \sqrt{2}b \quad (\text{A11})$$

when  $\kappa = -a/(1-b)$  or  $a/(1+b)$ ,

- and a part of the ellipse given by Eq. (A5) when  $\kappa \in (-a/(1-b), a/(1+b))$ .

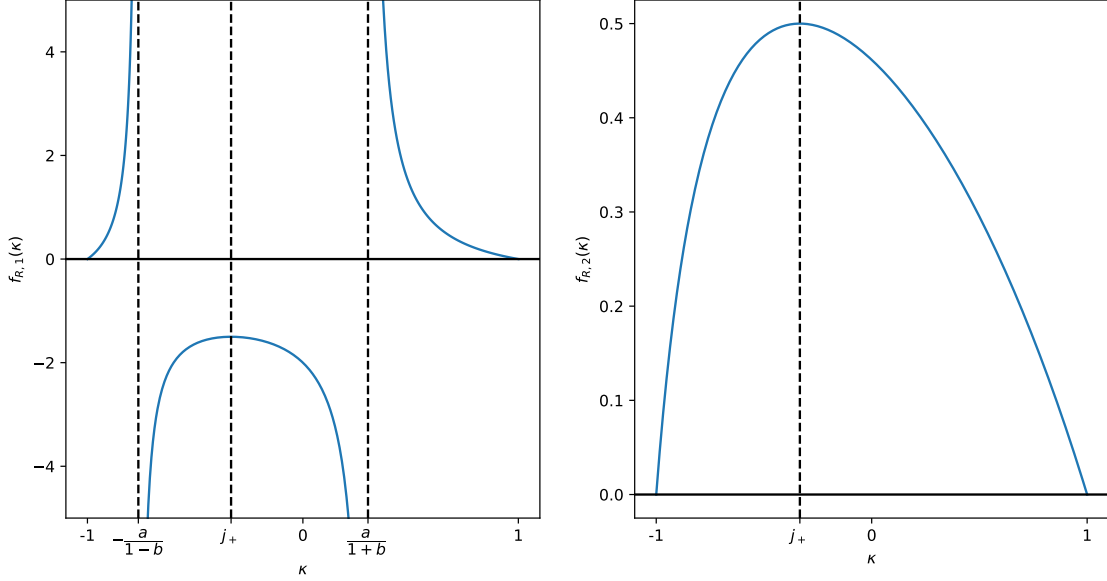
From Eq. (A9), a moving point on the line segment is mapped by  $\mathcal{U}$  to the endpoints when  $c_1 = \pm 1$  and  $c_1 = 0$ ; therefore, the endpoints are given as follows:

$$(u_1(\pm 1, \pm \kappa), u_2(\pm 1, \pm \kappa)) = \left( 0, \text{sgn}(s_2) \sqrt{\frac{2b^2(1-\kappa^2)}{1-(a-b\kappa)^2}} \right), \quad (\text{A12})$$

$$(u_1(0, 0), u_2(0, 0)) = \left( \text{sgn}(s_1) \sqrt{2}a, \text{sgn}(s_2) \sqrt{2}b \right). \quad (\text{A13})$$

The ellipse attains its maximum when  $\kappa = j_+$ , and the intersection with the  $u_2$ -axis at that time is  $\text{sgn}(s_2) \sqrt{f_{R,2}(j_+)}$ .

In the region mapped to a part of a hyperbola, we prove the following proposition:

FIG. 6. The graphs of  $f_{R,1}(\kappa)$  and  $f_{R,2}(\kappa)$ .

**Proposition 11.** *When  $\kappa$  varies over the interval  $(-1, -a/(1-b)) \cup (a/(1+b), 1)$ , the part of the hyperbola mapped by  $\mathcal{U}$  sweeps out the entire interior of the triangle in the  $u_1u_2$ -plane formed by the three points  $(0, 0)$ ,  $(+\sqrt{2}a, +\sqrt{2}b)$ , and  $(-\sqrt{2}a, +\sqrt{2}b)$ .*

*Proof.* It is sufficient to show that there exists  $\kappa$  in  $(-1, -a/(1-b)) \cup (a/(1+b), 1)$  when the variables  $(u_1, u_2)$  satisfy Eq. (A2) and exist in

$$\left\{ (u_1, u_2) \mid u_1 \in \left( -\frac{a}{b}u_2, \frac{a}{b}u_2 \right), u_2 \in (0, +\sqrt{2}b) \right\}. \quad (\text{A14})$$

We define the function  $g_R(\kappa)$  from the Eq. (A2) as follows:

$$g_R(\kappa) := -b^2\{\kappa^2 - (a - b\kappa)^2\}u_1^2 + a^2\{1 - (a - b\kappa)^2\}u_2^2 - 2a^2b^2(1 - \kappa^2). \quad (\text{A15})$$

we have  $g_R(-1) > 0$  because  $u_1^2 < (au_2/b)^2$ , and  $g_R(-a/(1-b)) > 0$  because  $u_2^2 < 2b^2$ . Since  $g_R$  is continuous in  $\kappa$ , there exists at least one  $\kappa$  in the interval  $(-1, -a/(1-b)) \cup (a/(1+b), 1)$  that satisfy  $g_R(\kappa) = 0$  by the intermediate value theorem. Therefore, the proposition holds.  $\square$

For the parameter  $\kappa$  of the curve passing through the point  $(u_1, u_2)$  on the  $u_1u_2$ -plane, since the function  $u_1(c_1, \kappa c_1)$  is monotonically increasing over  $c_1 \in [-1, 0]$ , and satisfies  $u_1(-1, -\kappa) \leq u_1(c_1, \kappa c_1) \leq u_1(0, 0)$ , it follows that there exists a corresponding  $c_1$  for  $(u_1, u_2)$ .

Hence, we obtain

$$\mathcal{U}(R) = \left\{ (u_1, u_2) \mid \frac{u_1^2}{-f_{R,1}(j_+)} + \frac{u_2^2}{f_{R,2}(j_+)} \leq 1 \right\} \cap \{ (u_1, u_2) \mid a|u_2| \geq b|u_1| \}. \quad (\text{A16})$$

Next, the discussion on  $\mathcal{U}(T)$  can be conducted almost in parallel with the discussion on  $\mathcal{U}(R)$ . Below, we list the corresponding equations to those that appeared in the discussion of  $\mathcal{U}(R)$ :

$$-b^2(1 - (a\gamma - b)^2)u_1^2 + a^2(\gamma^2 - (a\gamma - b)^2)u_2^2 = -2a^2b^2(1 - \gamma^2) \quad (\text{A17})$$

which corresponds to Eq. (A2),

$$f_{T,1}(\gamma) := \frac{2a^2(1 - \gamma^2)}{1 - (a\gamma - b)^2}, \quad (\text{A18})$$

$$f_{T,2}(\gamma) := \frac{2b^2(1 - \gamma^2)}{\gamma^2 - (a\gamma - b)^2}, \quad (\text{A19})$$

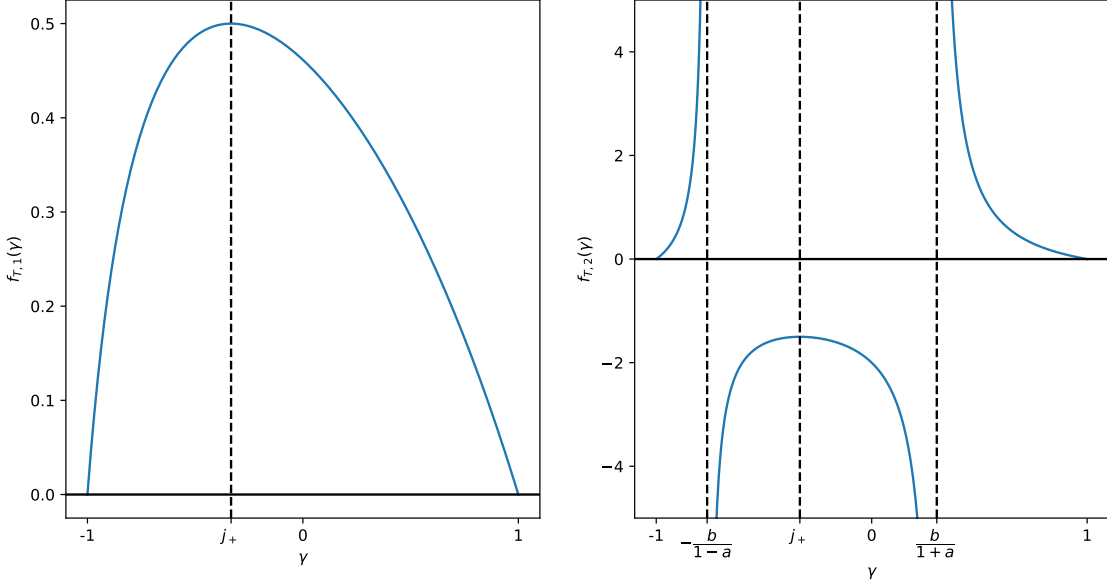
and

$$g_T(\gamma) := b^2(1 - (a\gamma - b)^2)u_1^2 - a^2(\gamma^2 - (a\gamma - b)^2)u_2^2 - 2a^2b^2(1 - \gamma^2), \quad (\text{A20})$$

and we show the graphs of  $f_{T,1}(\gamma)$  and  $f_{T,2}(\gamma)$  in FIG. 7. Therefore, we obtain

$$\mathcal{U}(T) = \left\{ (u_1, u_2) \mid \frac{u_1^2}{f_{T,1}(j_+)} + \frac{u_2^2}{-f_{T,2}(j_+)} \leq 1 \right\} \cap \{ (u_1, u_2) \mid a|u_2| \leq b|u_1| \}. \quad (\text{A21})$$

We have two ellipses in  $\mathcal{U}(R)$  and  $\mathcal{U}(T)$ . We need to analyze which ellipse is larger in the  $u_1$  and  $u_2$  directions,

FIG. 7. The graphs of  $f_{T,1}(\gamma)$  and  $f_{T,2}(\gamma)$ .

respectively. Thus, we calculate  $-f_{R,1}(j_+)$ ,  $f_{R,2}(j_+)$ ,  $f_{T,1}(j_+)$ , and  $-f_{T,2}(j_+)$ . The following equations are identities for all  $x \in \mathbb{R}$ :

$$\varphi(x) = x\{1 - (ax - b)^2\} - a(1 - x^2)(ax - b) \quad (\text{A22})$$

$$= x\{1 - (a - bx)^2\} + b(1 - x^2)(a - bx). \quad (\text{A23})$$

Because  $x = j_{\pm}$  are the solutions of  $\varphi(x) = 0$ , the following equations hold:

$$\frac{a(1 - j_{\pm}^2)}{1 - (aj_{\pm} - b)^2} = \frac{j_{\pm}}{aj_{\pm} - b} = \frac{1}{a - bj_{\mp}}, \quad (\text{A24})$$

$$\frac{b(1 - j_{\pm}^2)}{1 - (a - bj_{\pm})^2} = \frac{j_{\pm}}{a - bj_{\pm}} = \frac{1}{b - aj_{\mp}}. \quad (\text{A25})$$

We transform  $D_J$  as follows:

$$D_J = (1 + a^2 - b^2)^2 - 4a^2 \quad (\text{A26})$$

$$= (1 - a^2 + b^2)^2 - 4b^2, \quad (\text{A27})$$

We obtain the Eqs. (15)–(18) from the Eqs. (A3), (A4), (A18), (A19), and Eqs. (A24)–(A27), and the following inequalities hold:

$$-f_{R,1}(j_+) \geq f_{T,1}(j_+), \quad (\text{A28})$$

$$f_{R,2}(j_+) \leq -f_{T,2}(j_+). \quad (\text{A29})$$

Therefore, we obtain

$$\mathcal{U}([-1, 1]^2) = \mathcal{U}(R) \cup \mathcal{U}(T)$$

$$= \left\{ (u_1, u_2) \left| \frac{u_1^2}{-f_{R,1}(j_+)} + \frac{u_2^2}{f_{R,2}(j_+)} \leq 1 \right. \right\} \\ \cap \left\{ (u_1, u_2) \left| \frac{u_1^2}{f_{T,1}(j_+)} + \frac{u_2^2}{-f_{T,2}(j_+)} \leq 1 \right. \right\}, \quad (\text{A30})$$

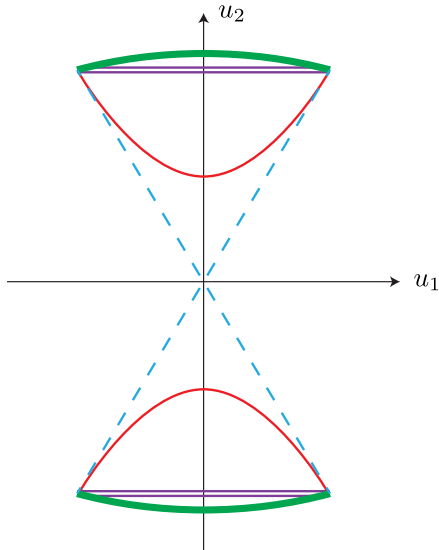
and  $\mathcal{U}([-1, 1]^2)$  is shown in FIG. 4. Finally, we obtain  $\sigma(\hat{v})$  from  $\mathcal{V} \circ \mathcal{U}([-1, 1]^2)$ .

## Appendix B: Detailed analysis of maps.

The signs  $-\text{sgn}(s_1)$  and  $-\text{sgn}(s_2)$  are lost when deriving Eq. (A1) from Eq. (42). Eq. (A2), which is derived from Eq. (A1), plays a central role in the analysis. As the parameter  $\kappa$  continuously moves from -1 to 1, the curves satisfying Eq. (A2) behave as described in FIG. 8.

When  $\kappa = -1$ , the curves lie on sky-blue dashed lines. As  $\kappa$  increases to the interval  $\kappa \in (-1, -a/(1-b))$ , the curves, which are segments of hyperbola, move along the upper and lower paths, shown as red solid curves in FIG. 8, when  $\kappa \in (-1, -a/(1-b))$ . At  $\kappa = -a/(1-b)$ , the curves become horizontal purple double lines. For  $\kappa \in (-a/(1-b), j_+)$ , the curves transition into segments of ellipses and move between the purple lines and green curves when  $\kappa \in (-a/(1-b), j_+)$ . When  $\kappa = j_+$ , the curves reach green thick curves. As  $\kappa$  exceeds  $j_+$ , the curves move back between the green curves and purple lines until  $\kappa$  reach to  $a/(1+b)$ . At  $\kappa = a/(1+b)$ , the curves once again form horizontal purple double lines. For  $\kappa \in (a/(1+b), 1)$ , the curves are segments of hyperbolas and gradually shift toward crossed sky-blue lines. Finally, when  $\kappa = 1$ , the curves return to the sky-blue dashed lines. To summarize, the line segment  $c_2 = \kappa c_1$ , which sweeps out the region  $R$  on  $c_1 c_2$ -plane, is mapped by  $\mathcal{U}$  and sweeps out  $\mathcal{U}(R)$  twice. In further detail, from Eq. (A9), a moving point on the line segment  $c_2 = \kappa c_1$ , from  $c_1 = -1$  to  $c_1 = 1$ , is mapped by  $\mathcal{U}$  and moves

FIG. 8. Movement of the curve which satisfies Eq. (A2).



from the intersection point with the  $u_2$ -axis to the point  $(\pm\sqrt{2}a, \pm\sqrt{2}b)$  when  $c_1 = 0$ , and then returns to the intersection point. The same analysis can be applied for the region  $T$  and its image  $\mathcal{U}(T)$ .

- 
- [1] J. Kempe, Quantum random walks - an introductory overview, *Contemporary Physics* **44**, 307 (2003), arXiv:quant-ph/0303081.
- [2] S. E. Venegas-Andraca, Quantum walks: A comprehensive review, *Quantum Inf. Process.* **11**, 1015 (2012).
- [3] N. Konno, Quantum random walks in one dimension, *Quantum Inf. Process.* **1**, 345 (2002).
- [4] G. Grimmett, S. Janson, and P. F. Scudo, Weak limits for quantum random walks, *Phys. Rev. E* **69**, 026119 (2004).
- [5] A. Suzuki, Asymptotic velocity of a position-dependent quantum walk, *Quantum Inf. Process.* **15**, 103 (2016).
- [6] N. Konno, Quantum Walks, in *Quantum Potential Theory*, edited by P. Biane, L. Bouten, F. Cipriani, N. Konno, N. Privault, Q. Xu, U. Franz, and M. Schürmann (Springer, Berlin, Heidelberg, 2008) pp. 309–452.
- [7] N. Inui, N. Konno, and E. Segawa, One-dimensional three-state quantum walk, *Phys. Rev. E* **72**, 056112 (2005).
- [8] C. Liu and N. Petulante, One-dimensional quantum random walks with two entangled coins, *Phys. Rev. A* **79**, 032312 (2009).
- [9] C. Liu, Asymptotic distributions of quantum walks on the line with two entangled coins, *Quantum Inf Process* **11**, 1193 (2012).
- [10] T. Miyazaki, M. Katori, and N. Konno, Wigner formula of rotation matrices and quantum walks, *Phys. Rev. A* **76**, 012332 (2007).
- [11] N. Konno, T. Luczak, and E. Segawa, Limit measures of inhomogeneous discrete-time quantum walks in one dimension, *Quantum Inf Process* **12**, 33 (2013).
- [12] K. Watabe, N. Kobayashi, M. Katori, and N. Konno, Limit distributions of two-dimensional quantum walks, *Phys. Rev. A* **77**, 062331 (2008).
- [13] C. Di Franco, M. Mc Gettrick, T. Machida, and Th. Busch, Alternate two-dimensional quantum walk with a single-qubit coin, *Phys. Rev. A* **84**, 042337 (2011).